

## Application of operating vehicle load to structural health monitoring of bridges

A.K.M. Rafiquzzaman<sup>†</sup> and Koichi Yokoyama<sup>‡</sup>

*Department of Urban & Civil Engineering, Ibaraki University, 4-12-1 Nakanarusawa,  
Hitachi, Ibaraki 316-8511, Japan*

*(Received April 27, 2005, Accepted October 14, 2005)*

**Abstract.** For health monitoring purpose usually the structure is instrumented with a large scale and multi-channel measurement system. In case of highway bridges, operating vehicle could be utilized to reduce the number of measuring devices. First this paper presents a static damage detection algorithm of using operating vehicle load. The technique has been validated by finite element simulation and simple laboratory test. Next the paper presents an approach of using this technique to field application. Here operating vehicle load data has been used by instrumenting the bridge at single location. This approach gives an upper hand to other sophisticated global damage detection methods since it has the potential of reducing the measuring points and devices. It also avoids the application of artificial loading and interruption of any traffic flow.

**Keywords:** structural health monitoring; damage detection; bridge; operating vehicle.

---

### 1. Introduction

The ability to continuously monitor the integrity of structures in real-time can provide for increased safety to the public, particularly for the aging structures in widespread use today. The ability to detect damage at an early stage can reduce the costs and downtime associated with repair of critical damage. Thus assessing damage is one of the main components of structural maintenance. Damages of civil engineering structures, such as highway bridges, including the degradation of columns, joints and beams, the breakage of braces, cumulative crack growth, impact by foreign object, fatigue etc., result in a sudden change of the stiffness and hence natural frequencies of the structures. Various approaches have been proposed in the literatures for detecting the damages in the structures (Doebling, *et al.* 1996, Chang 2004). In these studies, damages have been detected by a comparison of the system properties of damaged and undamaged structures.

Recently, methods based on signal decomposition have been proposed by the researchers to identify linear structures quite successfully (Yang and Lei 2000). They have used the vibration data in their signal processing. When the damage event occurs during the recording period of the health monitoring system, the recorded signal in the vicinity of the damaged location will have a discontinuity at that time or space instant. Such discontinuity can be detected through the data analysis techniques. A comparative study of damage

---

<sup>†</sup>Graduate Student, Corresponding author, [nd3304y@hcs.ipc.ibaraki.ac.jp](mailto:nd3304y@hcs.ipc.ibaraki.ac.jp)

<sup>‡</sup>Fellow of JSCE, Dr. Eng., Professor, [yokoyama@mx.ibaraki.ac.jp](mailto:yokoyama@mx.ibaraki.ac.jp)

identification algorithms applied to a test bridge was conducted by David, *et al.* In this study experimental modal data from a bridge were used. Damage index method, obtained from changes in mode shape curvature, performed best in detecting and localizing damages than other methods. In case of structural health monitoring of a bridge structure, in order to have vibration response data, it requires to close the lanes to apply any external forced vibration. Hence, It is necessary to direct the research of using bridge response induced by traffic operation by using ordinary vehicle instead of any external forced vibration and loading.

However, moving loads associated with roadway or railway traffic, induce significant dynamic effects in the structural behavior of bridges. Importance of this phenomenon has been stressed by different authors (Cantieni 1983, 1992, Billing 1984, Drosner and Sedlacek 1989, Hwang and Nowak 1991, Green, *et al.* 1995, 1997, Cole 1990, Cole and Cebon 1992, Wang, *et al.* 1992a,b, Humar, *et al.* 1993, 1995). The knowledge of actual vehicle load spectra for highway bridges is also essential for evaluation of the load carrying capacity, prediction of deterioration (corrosion), and remaining life (fatigue). An investigation of effect of truck-loads on bridges was carried out by Andrzej, *et al.* Establishment of live-load spectra and fatigue damage analysis for typical bridges was carried out by Ton-Lo, *et al.*

On the other hand, structural responses are usually measured by means of various gauges and sensors. For bridges, a large scale and multi-channel measurement system is required to grasp the whole structural behavior. However it is difficult to instrument the bridges with sensors at various locations, spatially if the structure is over the waterways or deep valley. At the same time it will be even more cumbersome to receive data from these locations as well as maintenances of the sensors regularly. In case of highway bridges, moving vehicle could be utilized in order to reduce the number of measuring devices. The influence line of the rotational angle and reaction forces at the support for the damaged and undamaged structure can be constructed from responses induced by operating vehicles. It has been found that maximum changes of rotational angle and reaction forces for pre and post-damaged structures occur at the damaged location. This concept has been used to localize damages of the structures. However, the applicability of the technique to field application remains at large. Dynamic noise and the effect of multi-axle vehicle loading problem with the data pose the major barrier towards its applicability to real field structures. This problem can be overcome by converting the dynamic data to static format by suitable filtering method. Multi-axle problem has been overcome by correcting the designated axle load to practically applied static load.

## 2. Localization of damage

To localize damage first the constituting parameters of a feature space (Musnitsky and White 1995) was constructed by forming indicators that are a function of measurable pre-damage and post damage structural parameters. Then the data are classified as damaged and undamaged by selecting an appropriate threshold value. Classifying the data through developing a decision algorithm can be used to choose this threshold value.

### 2.1. Developing feature space

#### 2.1.1. Using rotational angle

Damages in a bridge structure may occur in various forms like cracking, degradation of columns, joints and beams, the breakage of braces, cumulative crack growth, fatigue etc., result in a sudden change of flexural rigidity and natural frequencies of the structures. Damage usually occurs under

elastoplastic conditions. However, for particular type of damages like cracking and for limited vehicle loading (not heavily loaded) it can be assumed that Young's modulus  $E$ , of the element remains constant. Rather the Flexural rigidity  $EI$ , otherwise, moment of inertia ' $I$ ' of the damaged location changes. Hence, theory of superposition can be applied safely in this case. In case of nonlinear behavior of  $E$ , and in case of nonlinear damaged condition, principal of superposition should be applied carefully.

The structure of interest here has been modeled as a 1-D beam. Consider a moving load ' $P$ ' is applied on a simply supported beam as shown in Fig. 1 of length ' $L$ ' at a distance ' $a$ ' from the support  $A$ . Then the angle of rotation at that support is:

$$\theta_{A1} = \frac{Pa(L-a)(2L-a)}{6EIL} \quad (1)$$

Next, suppose the moment  $M_A$  is applied at support  $A$  of the same beam of Fig. 2. Deflection at distance ' $a$ ' is

$$\delta_{a2} = \frac{M_A a(L-a)(2L-a)}{6EIL} \quad (2)$$

Using reciprocal theorem,

$$P \cdot \delta_{a2} = \theta_{A1} \cdot M_A \quad (3)$$

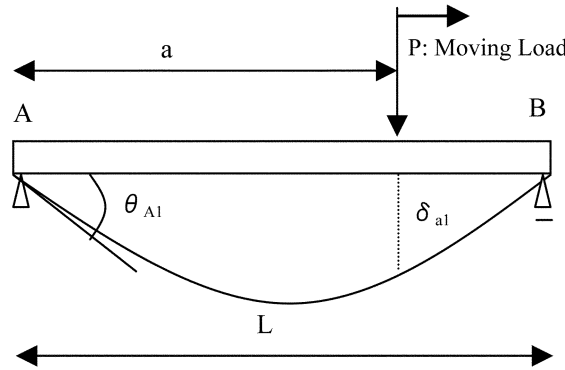


Fig. 1 Simple beam with moving load

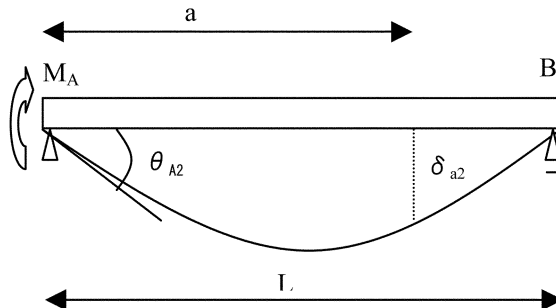


Fig. 2 Simple beam with applied moment

If numerical value of applied moment ' $M_A$ ' is equal to moving load ' $L$ ' then

$$\delta_{a2} = \theta_{A1} \quad (4)$$

Hence by measuring rotational angle at the support due to a moving load we can get the deflection curve of that structure. These values of deflection can in turn be used to find the structural property,  $EI$ . The instantaneous curvature  $v''$  at location ' $a$ ' along the length of the beam for the same beam (Fig. 1) will be:

$$v'' = \frac{M_a}{EI} \quad (5a)$$

where  $M_a$  is section moment at that section of beam. Curvature can be estimated from central difference operator (Pandey, *et al.* 1991) as

$$v''_l = \frac{\delta_{(l-1)} - 2\delta_l + \delta_{(l+1)}}{h^2} \quad (5b)$$

where  $h$  is the average distance between measurement points.  $v''_l$  is the curvature at point  $l$  and  $\delta_l$  is the displacement at point  $l$ .

From Eq. (5a) it is evident that curvature is directly proportional to the inverse of the bending stiffness,  $EI$ . If there is damage anywhere in the structure,  $EI$  will be reduced and accordingly curvature will be changed. Inversely, we can get the value of  $EI$  of the structure if the value of curvature is known for damaged and undamaged conditions.

$$EI_j = \frac{M_{aj}}{v_j} \quad (6a)$$

For a damaged

$$EI_j^* = \frac{M_{aj}}{v_j^*} \quad (6b)$$

We can get the damage index as:

$$\beta_j = \frac{EI_j - EI_j^*}{EI_j} \quad (7)$$

here asterisk (\*) stands for damaged case and subscript  $j$  stands for  $j$ -th node.

A preliminary study was conducted in the laboratory test to detect damage on a simple steel beam of 3.8 m long having damage at 1.7 m away from the left support. Static deflections due to a moving load were measured and the moment of inertia,  $I$  at those measured locations was calculated. Then damaged locations were predicted from differences between pre-damaged and post-damaged moment of inertia as shown in Fig. 3.

Since there is noise in the measurement, which affects the accuracy of damage identification, and since  $\beta_j$  seem to be normally distributed, we normalize these values as follows:

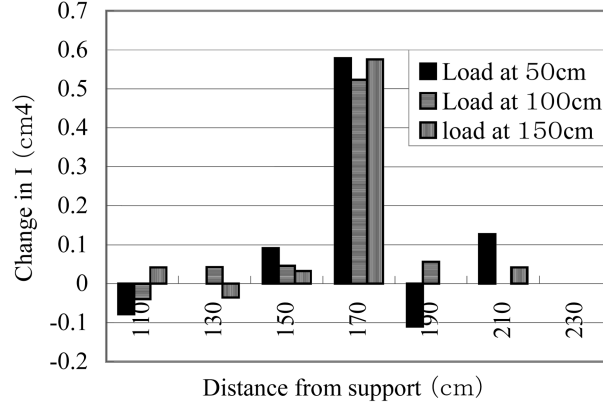


Fig. 3. Change in moment of inertia for load position at various points

$$Z_j = \frac{\beta_j - \mu_{\beta j}}{\sigma_{\beta j}} \quad (8)$$

where  $\mu_{\beta j}$  is the mean and  $\sigma_{\beta j}$  is the standard deviation of the sample values.

From simulations it has been confirmed that reciprocal theorem is also applicable to 2D and 3D structures. Hence, though for simplicity the theory have been developed by modeling the structure of interest as a 1-D beam. This approach is also applicable to other 2-D and 3-D structures like girder system or plates.

Responses at the supports can be measured with fare accuracy using smart bridge bearing integrated with composite load cells and fiber optic sensors or with other sort of smart sensors. A smart bridge bearing (Chase 2001) may detect and diagnose the distribution of live and dead loads to the bearings through structural system of the bridges. If there is a significant change in the flexural rigidity of a structural member through fracture, impact, or some other causes, it is likely that the distribution of the loads as well as the rotational angles of the bearing will change. Thus a smart bearing can be used to feel the damage in the bridge. This technology may be sophisticated in designing but concept is simple. And once designed it is easy to operate. These types of smart bearings and sensors are in the developing stage and yet to be commercially available in the market.

### 2.1.2. Using reaction forces

Let us consider a moving load ' $W$ ' is applied to a grid of beams of different flexural stiffness  $EI$  as shown in the Fig. 4 at a distance ' $x$ ' from the support  $A$ . Displacement at midspan of beam  $AB$ ,

$$\Delta_{c(AB)} = \frac{W(2L_1 - x)4L_1^2}{6EI_1} \left\{ (1 - \beta^2) \left( \frac{L_1}{2L_1} \right) - \left( \frac{L_1}{2L_1} \right)^3 \right\} - \frac{P(2L_1)^3}{48EI_1} \quad (9)$$

Displacement at the mid span of beam  $CD$ ,

$$\Delta_{c(CD)} = \frac{P(2L_2)^3}{48EI_2} \quad (10)$$

Since,  $\Delta_{c(AB)} = \Delta_{c(CD)}$  then

$$P = \frac{\left[ W(2L_1 - x)4L_1^2 \left\{ \frac{1}{2}(1 - \beta^2) - \frac{1}{8} \right\} \right]}{\left( \frac{L_1^3}{I_1} + \frac{L_2^3}{I_2} \right)} \quad (11)$$

Hence, reactions at support A and C

$$R_A = \frac{\{ W(2L_1 - x) - PL_1 \}}{2L_1} \quad (12)$$

$$R_c = \frac{P}{2} \quad (13)$$

Similarly, for damaged beam, P will be of different value, say,  $P^*$   
Hence, reaction for damaged case,

$$R_A^* = \frac{\{ W(2L_1 - x)(-P^*L_1) \}}{2L_1} \quad (14)$$

And damage index

$$\beta_j = |R_A - R_A^*| \quad (15)$$

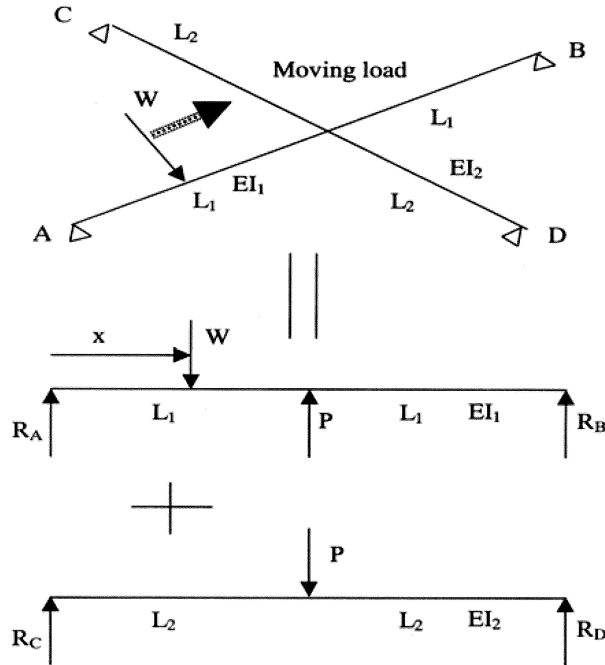


Fig. 4 A grid of beams of different stiffness

Normalizing the value we get,

$$Z_j = \frac{\beta_j - \mu_{\beta_j}}{\sigma_{\beta_j}} \quad (16)$$

From Eq. (11) it is evident that force  $P$  is dependent on stiffness of the structure. So the reduction in stiffness due to damage will eventually change the value of reaction forces. The maximum changes will occur when the moving load is at the damaged section

## 2.2. Classifying damages

A decision algorithm that would classify the feature space values into damaged and undamaged can be obtained in several ways, which include techniques from statistical pattern recognition, signal detection and classification analysis etc. Stubbs Norris, *et al.* chose pattern recognition technique to classify the damage pattern (Norris, *et al.* 1995). Here hypothesis technique was adopted to define data as damaged or undamaged. There are two hypothesis regarding values. The null hypothesis,  $H_o$ , assumes that the value of consists of noise only. In the alternative hypothesis,  $H_1$ , the location is assumed to be damaged.

Now, if we assume the knowledge of the probability density function (pdf) of the damaged and undamaged  $Z_j$ , we can use the Neyman-Pearson (NP) criterion as a classification algorithm. The NP detector uses a likelihood ratio test of the following form:

$$\lambda_T = \frac{p_1(z)}{p_o(z)} \geq \gamma \quad (17)$$

where,  $\lambda_T$  is the test static,  $z$  is the single observation of damage;  $p_1(z)$  is the pdf of  $z$  given that  $H_1$  is true;  $p_o(z)$  is the pdf of  $z$  given that  $H_o$  is true; and  $\gamma$  is a number which depends upon the significance level of test. The decision rule for NP detector is:

Choose  $H_1$ : when  $\lambda_T \geq \gamma$

Choose  $H_o$ : otherwise

An equivalent decision rule as shown in Fig. 5 simplifying to threshold limit  $K$  is:

Choose  $H_1$ : when  $Z \geq K$

Choose  $H_o$ : otherwise.

## 3. Numerical validation

To verify the theory described in section two, a number of simulations were performed from simple to complex structures. Simulation was done on three types of structures: 1-D simple beam, 2-D girder system and 3-D slab. Simple beam was chosen, as it is the simplest structural form for civil structures to simulate. Almost all of the previous researchers simulated a simple beam first to verify their theories of damage detection. Girder system was chosen as it represents the super structures of the bridge where the proposed method is intended to be used. As damage also occurs on to the bridge deck a slab was chosen for simulation. Physical dimensions of the structures are shown in Fig. 6 to Fig. 8. White noise at various ratios was incorporated with the simulated data.

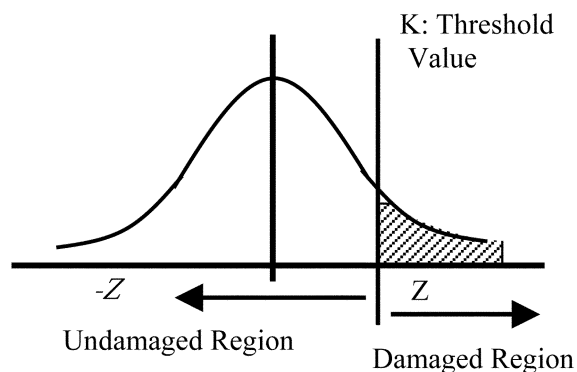


Fig. 5 Damage classification

### 3.1. Damage formulation

Damages in a bridge structure may occur in various forms like degradation of columns, joints and beams, the breakage of braces, cumulative crack growth, fatigue etc., result in a sudden change of stiffness and natural frequencies of the structures. Thus damage can be incorporated in the simulated structures by changing the material property, stiffness of the damaged element or by changing the element geometry, area. Here, in all three types of structures damage was introduced by reducing the thickness of elements by 10%. Actually, by reducing the thickness of the damaged element, we applied the reduction in flexural rigidity,  $EI$  at those damaged elements.

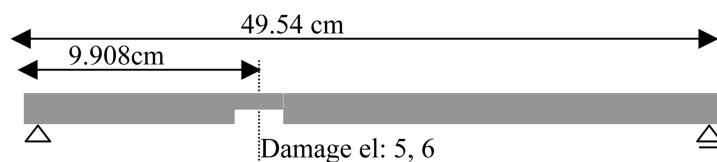


Fig. 6 Simple beam

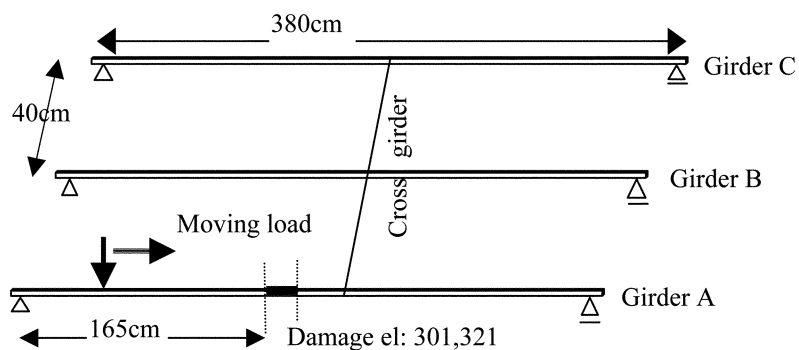


Fig. 7 Girder system



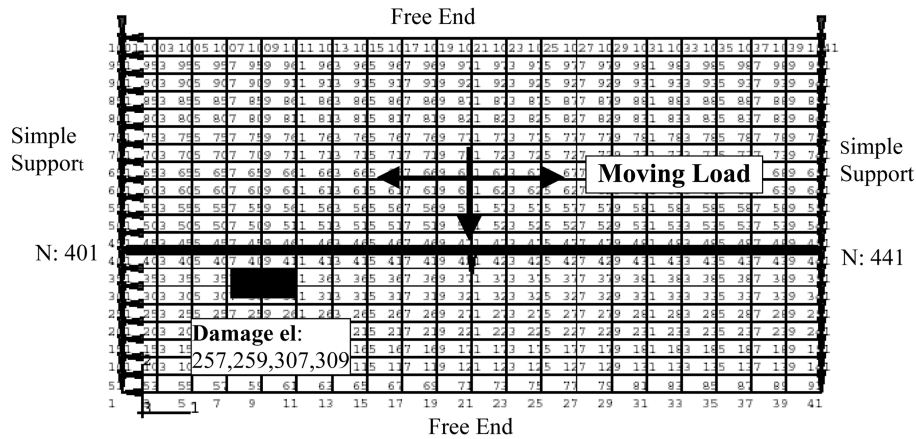


Fig. 8 Simple supported concrete slab with two free ends

### 3.2. Simulation results

#### 3.2.1. Simple beam

A moving load of 233.24 N has been applied on to the beam and the rotation of angle of both support have been calculated. The differences in rotational angles increase as the load moves from support towards the damage and reaches to its maximum value at the damaged section. Then further it decreases as the load moves from damaged section as shown in Fig. 9.

By using Eq. (4) we can assume displacements of the beam structure from where curvature can be calculated. Flexural rigidity for both damaged and undamaged cases was calculated by using Eq. (6a) and Eq. (6b). It has been found that maximum change in percentage of flexural rigidity is at node 6 (around 27%) where damage was introduced shown in Fig. 10.

To classify the locations of damage,  $\beta_j$  and  $Z_j$  were computed. The threshold value  $K$  from  $P_{fa} = 0.133$  whose corresponding normal value is 1.1 was also chosen. In Fig. 11 it is seen that  $Z_j$  of the nodes 5, 6 and 7, which comprised the damaged elements 5 and 6 are larger than threshold limit 1.10 specially the value of node 6 is more than 3.0. This node has been affected highly due to damage, as it is the middle

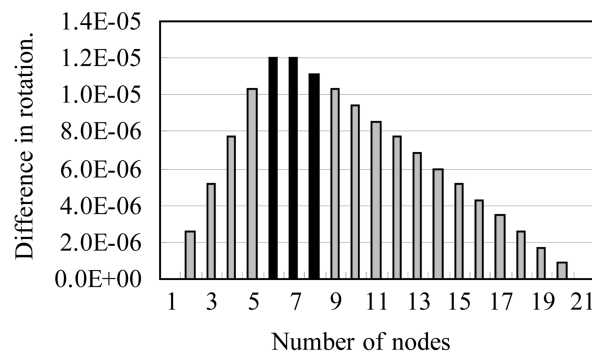


Fig. 9 Difference in rotation of support for simply supported beam

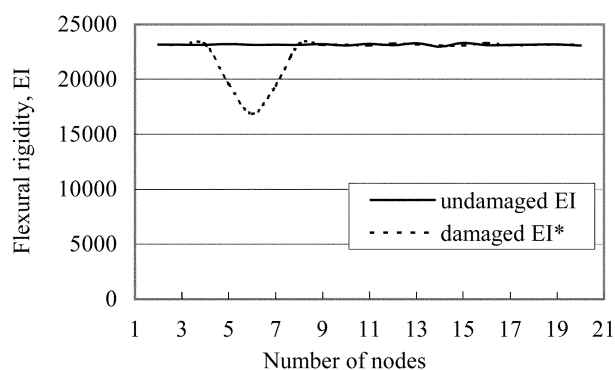


Fig. 10 Flexural rigidity, EI

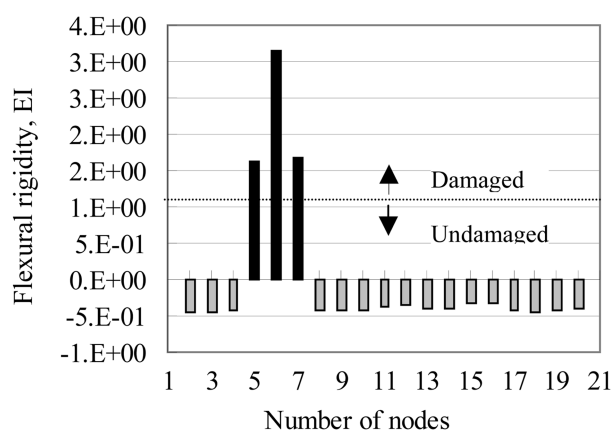


Fig. 11 Normal value of change in flexural rigidity, EI

node between two damaged elements. Other  $Z_j$  values are less than 1.10 indicating that these are undamaged nodes.

### 3.2.2. Girder system

Fig. 12 shows the percentage change in flexural rigidity of the girder A. It is seen that maximum change is at the damaged locations node 301 to node 341.

Fig. 13 and Fig. 14 show the normalized value of change in stiffness and reaction forces respectively. Maximum changed has been observed at the damaged location whose corresponding value is larger than the threshold limit.

### 3.2.3. Slab

A rectangular concrete slab as shown in Fig. 8 was modeled to understand the applicability of moving load in damage detection of a bridge deck. Damage was applied at elements 257, 259, 307, 309 consisting of nodes 257, 261, 357 and 361. Rotational angle and reaction forces at all nodes of the left support due to the moving load along the line (node 401 to node 441) from left to right were measured. Thus influence surfaces of absolute change in rotational angle and reaction forces at left support for the

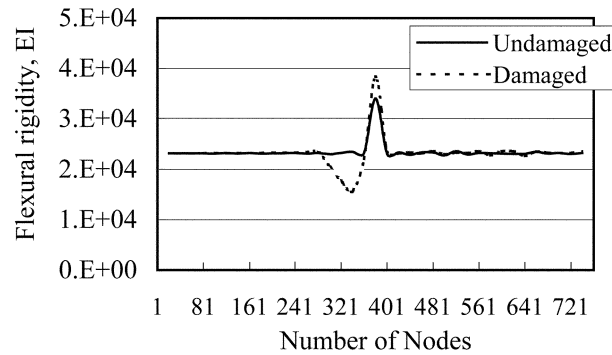


Fig. 12 Flexural rigidity, EI of girder A

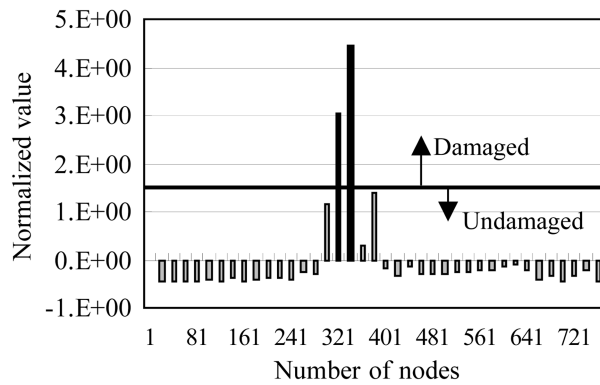


Fig. 13 Normalized value of change in flexural rigidity of girder A

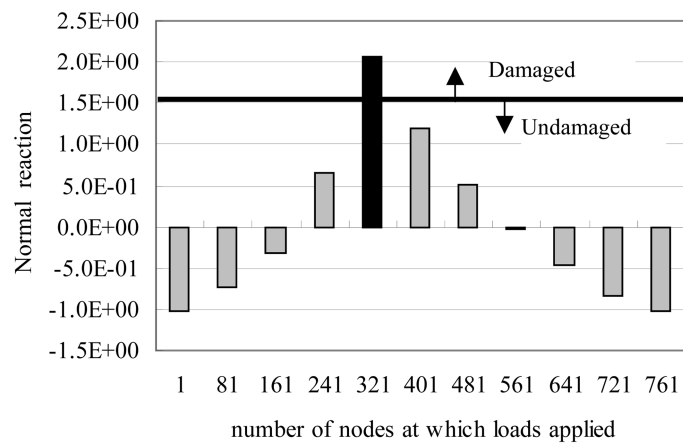


Fig. 14 Normalized value of difference in reactions

moving load along the line was constructed. It is seen that larger values are concentrated on the influence lines of rotational angle of nodes 201, 301 and 401 over the nodes of 207, 209, and 407, 409, which are located on and just around the damaged elements. This apparently suggests that damage position is along the line from node 301 to node 341. The moving load was then applied again along the

line of node 301 to node 341 and the influence surface of change in rotational angle and reaction forces were constructed as shown in Fig. 15 and Fig. 16. This confirms the damaged location more accurately as the values of change in rotational angles are larger than that of the previous Fig. 15, where moving load was applied along node 401 to node 441.

By using Eq. (4) to Eq. (6b) Flexural rigidity of the damaged and undamaged slab were then calculated. It is seen that maximum change in flexural rigidity occur when the load is at the damaged locations. The value of the change of flexural rigidity was converted to normalized value and threshold limit  $K=1.2$  was selected as  $P_{fa} = 0.122$ . Fig. 17 shows that normalized value of node 307, 309 and 311 are larger than the threshold limit 1.2, where damage was applied. Fig. 18 shows the normalized value of the damage index obtained from differences in reaction forces for the moving load from node 301 to 341. The value larger than the threshold limit localizes the damage. Similar simulations were done with simple beam and girder system incorporating various levels of noises. Table 1 shows the comparison of results within different types of structures and noises.

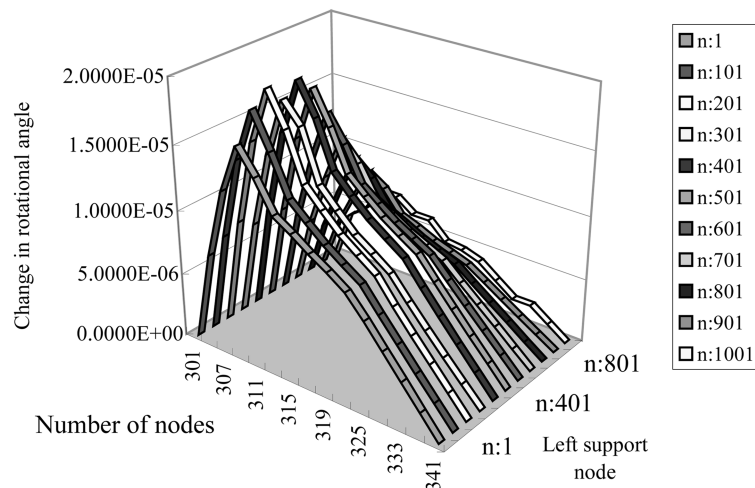


Fig. 15 Influence surface of absolute change in rotational angle at left upport for a moving load

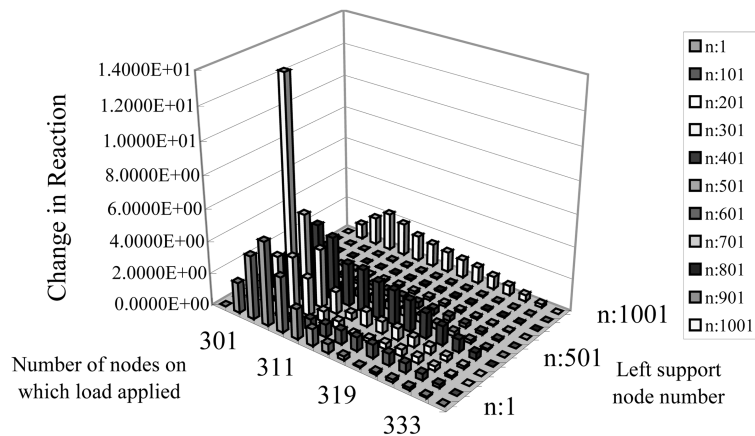


Fig. 16 Influence surface of absolute change in reaction at left support

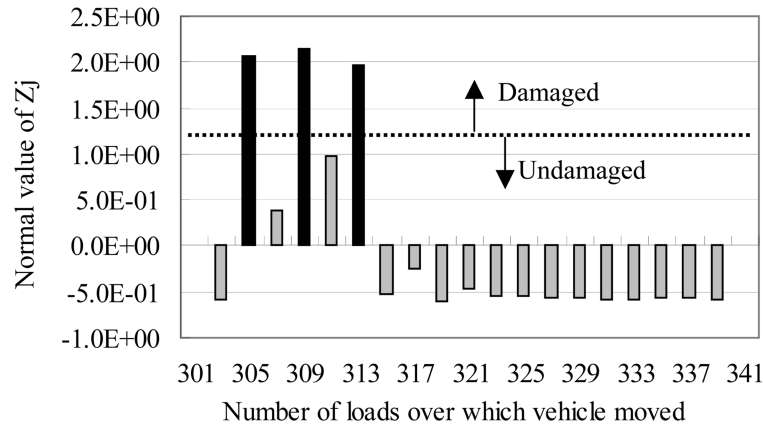
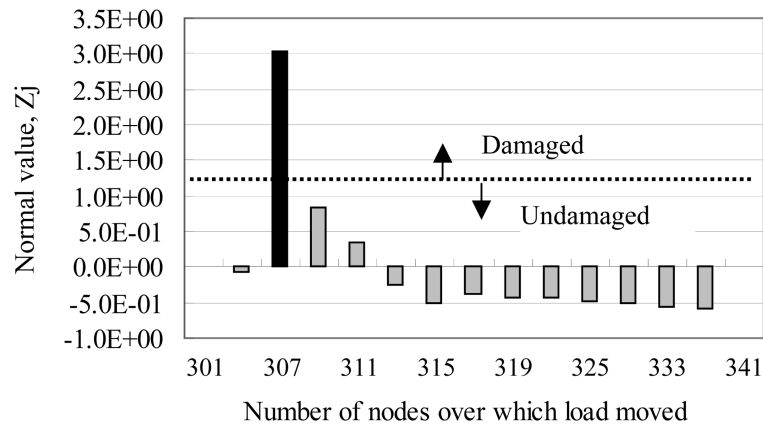


Fig. 17 Normalized value of percentage change in flexural rigidity

Fig. 18 Normal value of change in reaction at  $n: 301$ 

#### 4. Experimental results

In a preliminary study a laboratory test was conducted with the steel girder system to understand the applicability of reaction forces for damage detection. The geometry of the model was same as that of the model used in the simulation as shown in Fig. 7. Damages were introduced in the structure by cutting a rectangular slice from the girder. Tests were conducted by varying both the number and size of damages and by moving the load in different girders. Damage patterns are shown in Table 2. Reaction forces due to moving load were measured by instrumenting the system with load cells at the supports. The experimental data utilized a damaged detection scheme by instrumenting the structure at the support. Reaction forces of all the six supports were measured. Then a contributing reaction force factor at each support in relation to total reaction forces of the whole structure was calculated. The difference of the reaction force factor for damaged and undamaged structure was then plotted. From the pattern of the influence lines of these factors it is possible to predict the location of the damage. This result is particularly encouraging for the proposed method that it suggests about the practical applicability of operating vehicle load for damage detection. Fig. 19 shows the difference in reaction force factors for

Table 1 Comparison within different types of structures with different structural parameters

Structural Type	Structural Parameter	Noise level		
		0.00%	0.01%	0.10%
Beam	Rotation	Excellent	Good	Good
	Flexural rigidity	Excellent	Good	Cannot detect.
Multiple Girder	Reaction	Excellent	Good	Good. Nearby nodes are also affected
	Rotation	Excellent	Good	Good. Nearby nodes are also affected
	Flexural rigidity	Excellent	Good	Gives some false location also
Slab	Reaction	Excellent	Good	Good
	Rotation	Excellent	Good	Good
	Flexural rigidity	Excellent	Good	Gives some false location also

Table 2 Damage patterns and locations

Damage case	Damage on girder	Damage properties (cm)		
		Damage location	Damage length	Damage depth
1	A	95	15	0.3
2	A	175	15	0.3
3	B	95	15	0.3
4	B	175	10	0.3
5	B	175	15	0.3
6	A,B	175	15	0.3
7	A,C	175	15	0.3
8	A	95	15	0.6
9	B	95	15	0.6

the moving load on girder A. The values of the girder B are negative and the maximum difference is at a distance of 95 cm from the support. A 15 cm (Case 3) long real damage was applied on that location. Fig. 20 also localizes the damage at a distance of 175 cm on girder B where 10 cm (Case 4) long damage was applied.

## 5. Approaches to usage of bridge responses obtained from field observation

Before applying the proposed methodology in field, we need to apply some data analysis techniques to the noisy responses obtained from field observations. In the absences of any suitable filed data to verify the developed damage detection approach directly, this section explains an approach of using noisy bridge response induced by moving vehicle from field observation for health monitoring of bridges. Usually for structural health monitoring a large scale and multi channel measurement system is employed in highway bridges. Structural responses due to operating vehicle load of the bridges are measured with this measurement system. However, generally we face two major barriers with these data obtained from dynamic loadings while applying to damage detection algorithm. One of the two main problems of using this data is its dynamic noise component. Another problem with the operating vehicle load data is its multi axle loading effect. So to apply the damage detection algorithm to field

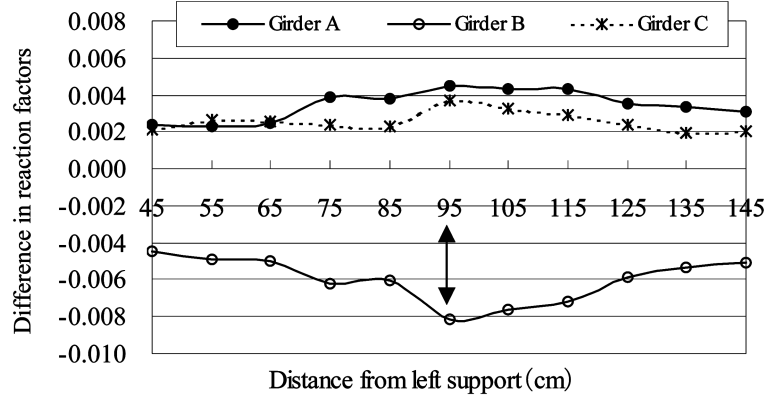


Fig. 19 Influence line of difference in reaction factors for the moving load on girder A

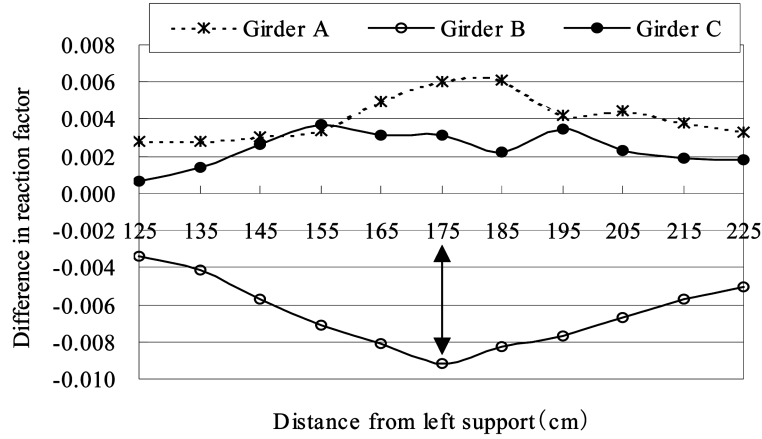


Fig. 20 Influence line of difference in reaction factors for the moving load on girder B

application, we need to find an approach of solving these two major problems associated with the dynamic data.

Due to dynamic interaction of vehicle and bridge deck and surface roughness, the measured response is wavy in nature as compared to static response as shown in Fig. 21. This fluctuative response can be transferred to usable data by applying Fast Fourier Transformation (FFT) or other filtering method. Hanning Window can also be used as an appropriate method for converting the dynamic data to static data. The following equation can be used repeatedly until the wavy nature of the graph smoothens out.

$$X_i = \frac{1}{4}x_{i-1} + \frac{1}{2}x_i + \frac{1}{4}x_{i+1} \quad (18)$$

Where,  $X_i$  is the converted static response and 'i' is the measuring points. It can be mentioned here that the number of repetitions of using Eq. (18) depends on the extent of fluctuation of the measured data. The second problem lies with the compliance of the multi axle load of the vehicle and corresponding response, say, strain. It has been found that due to the arrangement of the axles, practically applied vehicle load is usually smaller than the total weight of the vehicle. So to make the static strain matching

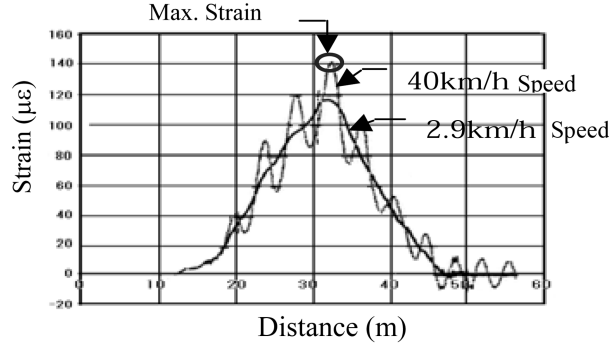


Fig. 21 Dynamic Vs. Static strain

to corresponding vehicle load the following equation based on the influence line can be used to correct the applied axle load.

$$X = \frac{\varepsilon_w * W}{\varepsilon_x} \quad (19)$$

where,  $X$  (ton) is the effective vehicle load.  $\varepsilon_w$  is the corresponding calculated strain due to single weight  $W$  (ton).  $\varepsilon_x$  is the converted strain of the due to the moving vehicle over the bridge structure.

In this paper Weigh-In-Motion (WIM) data of Miyanogi Bridge, Japan as shown in Fig. 22 has been used to show the applicability of operating vehicle load data to structural health monitoring of bridges. Before instrumenting for health monitoring, the bridge has been retrofitted and strengthened in three phases beginning from the end of year 1994 to mid of 1995 by adding additional girder No 4, cover plate under girders and thickening the deck respectively. A total number of 30 strain gauges and 2 temperature sensors have been installed. A Loop type WIM system has also been embedded for monitoring the vehicle load. Dynamic strain data due to the moving vehicle is being measured in every 0.05 second (20 Hz).

Among numerous data, the strain data measured at girder No 2 with corresponding WIM data has been used in this case. The wavy nature of the strain data has been smoothened out by using Hanning Window equation. The correlation coefficient between the converted static strain and vehicle weight has been found at around 0.8 as shown in Fig. 23. It implies a somewhat inferior agreement between these two factors. Using the corrected effective vehicle load by applying the Eq. (19), a high correlation coefficient (0.9009) has been found with converted static strain as shown in calibration graph in Fig. 24. Similar high correlation coefficients greater than 0.90 have been found with the data measured at other locations in other girders. This calibration graph can be used to monitor the abnormal strain of the girder due to the moving vehicle load. In other way, from this converted static strain corresponding displacement and stress of the component can be calculated and thus can be used as a tool for health monitoring purposes. By using the reciprocal theorem displacement at one location for a running vehicle can be used to find the displacement of the entire structure. This can be used to localize the damage with comparing to the data of the intact structure. Japan Highway Public Corporation monitored the strain and stress of the bridge over the years as shown in Fig. 25. It is clear that maximum stress has been reduced due to strengthening the bridge by adding additional girder, cover plate and by thickening the deck. After the full repair, health monitoring system was installed in order to clarify the effectiveness of strengthening and monitoring the response of the bridge as it grows old. Thus for health



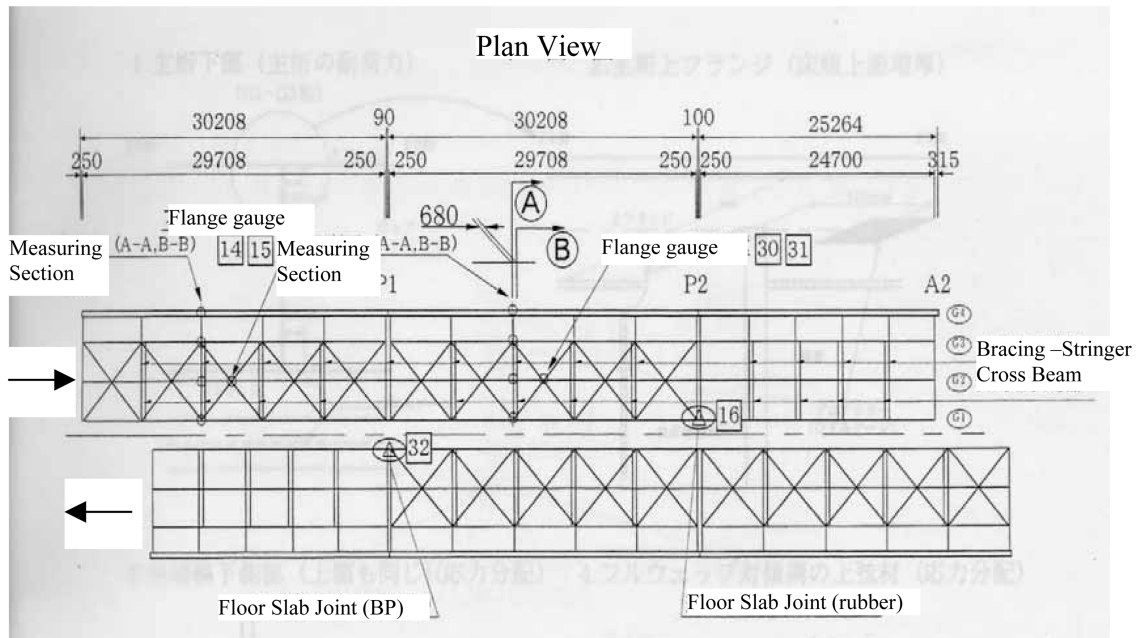


Fig. 22 Plan view of Miyanogi Bridge

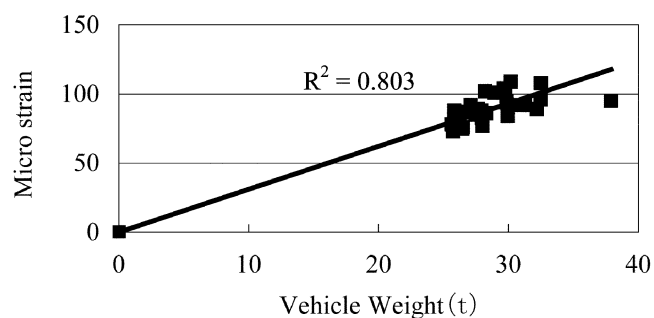


Fig. 23 Strain vs weight of the vehicle

monitoring, 1995 data obtained after the complete strengthening can be used as reference year. During its service life if the maximum stress reaches at a certain level, it can be assumed that the bridge has got damage corresponding to Fig. 25.

## 6. Conclusions

The proposed health monitoring approach developed in this research uses the static local damage detection algorithm using operating vehicle load. The basic theory of the method has been validated by numerical simulations with various types of structures with different levels of noises. Small-scale laboratory test also shows the applicability of the technique. To show the extension of the technique to field application, responses measured at Miyanogi Bridge has been

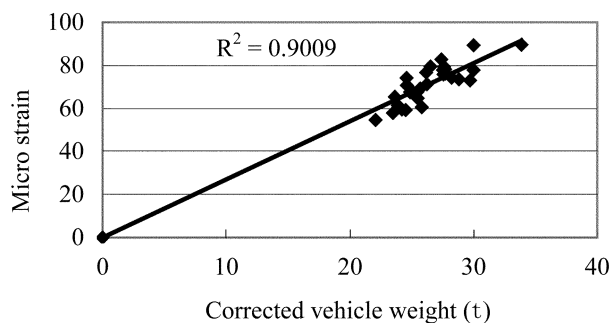


Fig. 24 Strain Vs. corrected weight of the vehicle

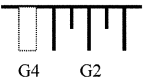

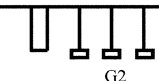
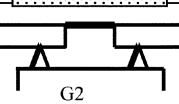
Without Girder 4 Year	Addition of Girder 4	Addition of Cover plate	Thickening of Bridge deck	Monitoring
1992.2	1994.12	1995.2	1995.6	1998.12~1999.3
				
Max. stress 51.5	37.1	28.1	19.1	24.0
Min stress -30.8	-3.7	-2.9	-3.9	-1.0
Difference 82.3	40.8	31.0	23.0	25.0
*Stress in MPa				

Fig. 25 Monitoring of stresses of Miyanogi bridge

used. Here the approach has been found out to overcome the barriers associated with the applicability of the noisy data and multi-axle vehicle-loading problem. Noisy dynamic data can be transferred to static data to be usable to local damage detection algorithm and to assess the health of the structure.

This damage detection technique can reduce the anxiety of the owners and engineers since it minimizes the number of required sensors and measurement difficulties, which gives an upper hand to other sophisticated global damage detection methods. Using operating vehicle load response of bridges for structural health monitoring will also reduce the burden of closing lanes of busy highway bridges.

### Acknowledgements

The authors are indebted to Japan Highway Public Corporation for providing the data of Miyanogi Bridge. Contribution for material resources from the research group comprising Hosoda Takeshi, Shimada Hiromitsu and Eriko Yoshizawa, Department of Urban and Civil Engineering, Ibaraki University, Japan is also gratefully acknowledged.

## References

- Andrzej S. Nowak, Hani Nassif, and Leo DeFrain (1993), "Effect of truck loads on bridges", *J. Trans. Eng.*, **119**(6), 853-867.
- Cantieni, R. (1983), "Dynamic load tests on a highway bridges in Switzerland-60years experience of EMPA", EMPA Report No 211, Swiss Federal Laboratories for materials Testing and Research, Switzerland.
- Cantieni, R. (1992), "Dynamic behavior of highway bridges under the passage of heavy vehicles", EMPA Report No 220, Swiss Federal Laboratories for materials Testing and Research, Switzerland.
- Chang, F. -K. (2004). *Proc., 4th, Int. Workshop on Structural Health Monitoring*, Stanford Univ., Stanford, California. (DEStech Publication Inc., Pennsylvania, USA).
- Cole, D. (1990), "Measurement and analysis of dynamic tyre forces generated by lorries", PhD thesis, Cambridge Univ., England.
- Cole, D. and Cebon, D. (1992), "Validation of an articulated vehicle simulation", *Veh. Syst. Dyn.*, **21**, 197-223.
- David V. Jauregui and Charles R. Farrar, "Comparison of damage identification algorithms on experimental modal data from a bridge", Los Alamos National Laboratory, Los Alamos, NM 87545, USA
- Doebeling, S. W., Farrar, C. R., Prime, M. B., and Shevitz, D. W. (1996), "Damage identification and health monitoring of structural and mechanical system from changes in their characteristics", *A Literature Review. Rep. LA-13070-MS, Los Alamos national laboratory*, Los Alamos, N.M.
- Green, M. F., Cebon, D., and Cole, D. J. (1995), "Effects of vehicle suspension design on dynamics of highway bridges", *J. Struct. Eng.*, **121**(2), 272-282.
- Green, M. F., and Cebon, D. (1997), "Dynamic interaction between heavy vehicles and highway bridges", *Comput. Struct.*, **62**(2), 253-264.
- Humar, L., and Kashif, A.M. (1993), "Dynamic response of bridges under traveling loads", *Can. J. Civ. Eng.*, **20**, 287-298.
- Humar, L., and Kashif, A.M. (1995), "Dynamic response analysis of slab-type bridges", *J. Struct. Eng.*, **121**(1), 48-62.
- Hwang, E.-S., and Nowak, A. S. (1991), "Simulation of dynamic load for bridges", *J. Struct. Eng.*, **117**(5), 1413-1433.
- Musnitsky, J. and White, K. R. (1995), "Korean bridge inspection evaluation".
- Pandey, A.K., Biswas, M. and Samman, M.M. (1991), "Damage detection from changes in curvature mode shapes", *J. Sound Vib.*, **145**(2), 321-332.
- Chase, S. B. (2001), "High-tech inspection", *Civil Engineering*, September.
- Norris, S., Kim, J.-T. and Farrar, C. R. (1995), "Field verification of a nondestructive damage localization and severity estimation algorithm", *Proceedings 13<sup>th</sup> International Modal analysis Conference*, Nashville, TN.
- Wang, T.-L., Liu, C., Huang, D. and Shahawy, M. (2005), "Truck loading and fatigue damage analysis for girder bridges on Weigh-in-Motion data", *J. Bridge Eng.* **10**(1), 12-21.
- Wang, T.-L., and Huang, D (1992a), "Cable-stayed bridge vibration due to road surface roughness", *J. Struct. Eng.*, **118**(5), 1354-1374.
- Wang, T.-L., Huang, D. and Shahawy, M. (1992b), "Dynamic response of multigirder bridges", *J. Struct. Eng.*, **118**(8), 2222-2238.
- Yang, J. N. and Lei, Y. (2000), "System identification of linear structural dynamics", *Society for Experimental Mech.*, **1**, 213-219.